Tip Position Control Of Flexible Arms Using A Control Law Partitioning Scheme

Kuldip S. Rattan

Department of Electrical Engineering
Wright State University
Dayton, OH. 45435

Vincente Feliu[1] and H. Benjamin Brown Jr.

Robotics Institute
Carnegie Mellon University
Pittsburgh, Pennsylvania 15213

Abstract

Tip position control of a flexible arm with friction in the joints is carried out in this paper. The control scheme is based on two nested feedback loops, an inner loop to control the position of the motor and an outer loop that controls the tip position of the flexible arm. The inner loop is controlled by a high gain controller to remove the effects of friction. A control law partitioning scheme that partition the control law into a model-based portion and a servo portion, is used for the control of the outer loop. To make the arm follow the desired trajectory without any delay, a feedforward term is added to the control law. The control scheme is experimentally evaluated on two very lightweight flexible arms.

1 Introduction

The tip position control of flexible arms with friction in the joints is carried out in this paper using the control law partitioning scheme. The control scheme is based on the general robust control scheme proposed by Rattan et al. [3] that overcame the effects of friction in the joints. This scheme (Figure 1) is composed of two nested feedback loops, an inner loop to control the position of the motor (θ_m) and an outer loop for the tip position (θ_t). It was shown that the use of a high gain controller in the inner loop removes the effects of friction. Once this is achieved, the inner loop may be represented (for tip position control purposes) as a linear system with constant coefficients whose input is the desired angle of the motor (θ_{mr}) and whose output is the actual angle of the motor (θ_m).

Another important result obtained by closing the inner loop with a high gain controller is that the response of the inner loop is much faster as compared to the dynamics of the mechanical beam. This means that the inner loop may be represented by a unity transfer function for the sake of analysis and design of the outer loop. This is especially true in lightweight flexible arms. But, when the reaction torque of the flexible arm is comparable to the motor input torque, this assumption no longer remains true. However, it may still be used as an approximation in the design of the tip position control loop, and correction terms may be added later in order to compensate for the delays that appear in the response of the servo-controlled motor.

If we assume that the previous statement is true, the only dynamics that needs to be considered for the design of the tip position loop is the transfer function of the beam, $G_b(s)$ (Figure 1), which relates the angle of the motor (input) to the tip position (output). Once this is done, either the classical or modern control techniques may be used to design a controller for the outer loop.

In this paper, the tip position control loop is controlled by a control law partitioning scheme (Craig [6], Khosla and Kanade [2]). In this scheme, the control law is partitioned into a model-based portion and a servo portion. For the flexible beam with one vibration mode, $G_b(s) = \omega_n^2/(s^2+\omega_n^2)$, the model-based portion of the control law is obtained by simply closing a positive unity feedback loop around the tip position and pre-multiplying by a gain factor, $1/\omega_n^2$. This has the effect of cancelling the vibration mode of the beam and reducing the dynamics of the beam to a double integrator. Once this is done, a servo portion of the control law can be designed which is independent of the dynamics of the beam. To make the beam follow a reference trajectory without any delay, a feedforward term which is the second derivative of the reference position can be added to the control law. This simple scheme is best suited for flexible beams with one vibration mode and is not directly applicable to beams with more than one vibration mode. In this paper, we have extended this scheme to flexible beams with two vibration modes. In the case of beams with more than one vibration mode, the positive unity gain feedback loop removes the first (dominant) vibrating mode, independent of the transfer function of the beam. This is then pre-multiplied by the inverse of the minimum phase portion of the resultant transfer function (transfer function of the flexible beam after closing the positive unity feedback loop around the tip position). The feedforward term for this scheme also contains terms to compensate for the minimum phase portion of the simplified transfer function of the beam.

The paper is organized as follows. The control of the inner loop is briefly described in section 2. Section 3 discusses the design of the tip position control loop. A brief description of the control law partitioning scheme and the design of the feedforward term is also given in section 3. These results are applied to two experimental systems, a single-mass arm and a two-mass arm, in section 4. The performance data of the two arms are presented. Some conclusions are drawn in section 5.

2 Motor Position Control Loop

The motor position control loop corresponds to the inner loop of Figure 1. We want to achieve two objectives when designing

[1]Visiting Professor, Dpto Ingeniería Eléctrica, Electrónica y Control, UNED, Ciudad Universitaria, Madrid-28040, Spain

CH2876-1/90/0000/1803$01.00 © 1990 IEEE

a controller for this loop:

1. remove the modelling error and the nonlinearities introduced by Coulomb friction and changes in the coefficient of the dynamic friction,

2. make the response of the motor position much faster than the response of the tip position control loop (outer loop in Figure 1).

The fulfillment of the second objective allows us to substitute the inner loop by an equivalent block whose transfer function is approximately equal to one, i.e., the error in motor position is small and is quickly removed. This simplifies the design of the outer loop as illustrated in the next section. The differential equation relating the angle of the motor to the applied current can be written as

$$Ki = J\frac{d^2\theta_m(t)}{dt^2} + V\frac{d\theta_m(t)}{dt} + C_t(t) + \text{CF} \qquad (1)$$

where K is the electromechanical constant of the motor, i is the current of the motor, $\theta_m(t)$ is the angle of the motor, J is the polar moment of inertia of the motor and hub, V is the dynamic friction coefficient, $C_t(t)$ is the coupling torque between the motor and the link (the bending moment at the base of the link), CF is the Coulomb friction and t is time.

To simplify the design of the inner loop, the system described in equation (1) can be linearized by compensating for the Coulomb friction, and decoupled from the dynamics of the beam by compensating for the coupling torque. This is done by adding, to the control current, the current equivalent to these torques (Figure 2) and is given by

$$i_c(t) = (C_t(t) + \text{CF (sign of motor velocity)})/K \; . \qquad (2)$$

The magnitude of the Coulomb friction, CF, is identified from the spectral analysis of the motor position and the current signals. The details of the identification method can be found in [5]. The coupling torque $C_t(t)$ can be calculated either from strain gauge measurements at the base of the link or by the difference of the measurements of the angles of the motor and tip. The second approach is used in this paper. Since the single-mass beam is nearly massless, we can assume that the coupling torque $C_t(t) = C(\theta_m(t) - \theta_t(t))$, where C = (3.E.I)/L is a constant that depends on the stiffness (E.I) and length L of the arm. For a two-mass beam, the coupling torque is more complex as compared to the single-mass case. But because of the limited computational capabilities of the microprocessor used for this study, a simpler coupling term of the form $C_t(t) = \hat{C}(\theta_m(t) - \theta_t(t))$ was implemented. After compensating for the friction and coupling torque, the transfer function between the angle of the motor and the current can be written as $G_m(s) = \theta_m(s)/i(s) = (K/J)/s(s + V/J)$.

The block diagram of the inner loop control system is shown in Figure 2 (discrete control version). The series and feedback controllers (G_{c1} and G_{c2}, respectively) are designed so that the response of the inner loop (position control of the motor) is significantly faster than the response of the outer loop (position control of the tip) and without any overshoot. This is done by making the gain of the series controller large and is limited only by the saturation current of the servo amplifier. It was shown in [3] that, in theory, this gain could be made arbitrarily large even in the case of the arm being a nonminimum phase system. It was also shown that large gain in this loop reduce the effects of nonlinearities caused by friction.

When the closed-loop gain of the inner loop is sufficiently high, the motor position will track the reference position with small error. The dynamics of the inner loop may then be approximated by '1' when designing the outer loop controller.

3 Tip Position Control Loop

The proposed control scheme for the tip position is composed of two loops: a loop containing the model-based portion of the control law and a servo loop containing a classical proportional plus derivative (PD) controller as shown in Figure 3. A feedforward term is added to the tip position control system to make the tip response follow the reference trajectory without any delay. We assume here that the inner loop has been closed to minimize the effects of friction and coupling torque. When the response of the inner loop is much faster than that of the outer loop, the motor closed-loop transfer function can be assumed to be unity.

Control law partitioning scheme with a feedforward term has been used in the control of rigid arms (Craig [6], Khosla and Kanade [2]). In this schemes, the feedforward term generates a torque (current) to drive the arm that is a function of the desired trajectory and the model-based portion of the control law generates a torque to compensates for the dynamics of the beam. The servo control loop compensates for the tracking errors produced by perturbations. Our feedforward term differs from the existing methods in that it uses motor angle rather than the torque as the generated signal. Thus, the feedforward term may be defined as the second derivative of the reference trajectory. For a beam with two vibration modes, transfer function of the feedforward term also contains terms to compensate for the minimum phase portion of the beam transfer function. The feedforward term used for this method is simpler than the terms generated in the above mentioned methods and can be easily computed in real-time.

3.1 Model-Based Control Loop

The purpose of this loop is to simplify the dynamics of the arm. The model-based loop for both single-mass flexible arm (one vibration mode) and two-mass flexible arm (two vibration modes) will be discussed below.

3.1.1 Single-Mass Flexible Arm

For the case of a flexible beam with only one vibrational mode, a very simple model-based loop can be implemented that reduces the dynamics of the system to a double integrator. This is done by simply closing a positive unity gain feedback loop around the tip position. Provided that the inner loop has been satisfactorily closed, the transfer function of a lightweight flexible arm with one vibration mode ($G_b(s)$ in Figure 1) can be written as

$$G_{b1}(s) = \frac{\omega_n^2}{s^2 + \omega_n^2} \quad . \qquad (3)$$

The natural resonant frequency of the beam with the motor fixed is ω_n rad/sec. and is related to the constant C, the load at the tip m and the length L by the expression $\omega_n^2 = C/mL^2$.

By closing a positive unity gain feedback loop around the tip position, expression (3) is transformed into ω_n^2/s^2 and is then multiplied by $G_{bd1}(s) = 1/\omega_n^2$ to reduce the dynamics of the beam to a double integrator (Figure 3). Thus, the transfer function of the reduced system is given by

$$G'_{b1}(s) = \frac{1}{s^2} \quad . \tag{4}$$

3.1.2 Two-Mass Flexible Arm

The transfer function of a two-mass flexible arm with two vibration modes can be written as

$$G_{b2}(s) = \frac{K_{b2}(a^2 - s^2)}{(s^2 + \omega_{n1}^2)(s^2 + \omega_{n2}^2)} \tag{5}$$

where ω_{n1} and ω_{n2} are the natural frequencies of the two vibration modes. Also, for the final position of the tip to be the same as the position of the motor, $K_{b2}a^2 = \omega_{n1}^2\omega_{n2}^2$. By closing a positive unity gain feedback loop around the tip position, the transfer function given by (5) is transformed into $\frac{K_{b2}(a+s)(a-s)}{s^2(s^2+b^2)}$, where $b = K_{b2} + \omega_{n1}^2\omega_{n2}^2$. This is then multiplied by $G_{bd2}(s) = \frac{s^2+b^2}{K_{b2}(s+a)}$ (Figure 3) to reduce the dynamics of the beam into

$$G'_{b2}(s) = \frac{a - s}{s^2} \quad . \tag{6}$$

3.2 Feedforward Term

A general expression for the feedforward term was derived by Feliu et al. [5] and is given by

$$\hat{G}_b(s) = \frac{s^3}{G_b^+(s)} \left| \frac{G_b(-s)}{G_b^-(s)s^3} \right|_+ \tag{7}$$

where $G_b(s)G_b(-s) = G_b^+(s)G_b^-(s)$. $G_b^+(s)$ and $G_b^-(s)$ group all the poles and zeros of $G_b(s)G_b(-s)$ that are in the left and right half-planes respectively.

3.2.1 Single-Mass Flexible Arm

A feedforward acceleration term for the single-mass flexible arm that makes the tip follow the reference without any delay is given by

$$Feedforward1(s) = s^2\theta_{tr}(s) \tag{8}$$

where $\theta_{tr}(s)$ is the Laplace transform of the commanded trajectory profile for the tip. Notice that (8) uses the second derivative of the reference position. It means that parabolic profiles of at least order two must be used as reference signals in this scheme.

3.2.2 Two-Mass Flexible Arm

Using the expression given in (7), a feedforward term for the flexible beam with two vibration modes can be obtained as

$$Feedforward2(s) = (s^2 + \frac{2}{a}s^3 + \frac{2}{a^2}s^4)\frac{1}{s+a}\theta_{tr}(s) \; . \tag{9}$$

Equation (9) uses the fourth derivative of the reference input. Therefore, a quasi-parabolic trajectory of at least order four must be used as a reference input to the flexible arm.

3.3 Servo Control Loop

As mentioned before, the use of a feedforward term allows us to simplify the design of the servo controller. Generally, a proportional plus integral plus derivative (PID) controller is used as a servo controller. However, since the compensation for the Coulomb friction was provided in the inner loop, the servo controller may even be simpler because the integral action is not needed. This allows us to use high sampling rates improving the general behavior of the digital control system.

The design of the servo controller can be carried out using the classical frequency domain techniques or more sophisticated modern control techniques. To move the arm to the desired angle, most of the control action is provided by the feedforward term. The function of the servo controller is to compensate for the deviation of the tip position from the desired trajectory. It is well known that the poles of a plant of the form (4) or (6) can be perfectly placed by using a simple PD controller (Kuo [7]). Let us express this controller as $G_{c3}(s) = K_P + sK_D$.

The resulting control scheme after closing loops described in sections 3.1. and 3.2. is shown in Figure 3. If the load at the tip were constant, this scheme would provide a nearly perfect trajectory tracking and error compensation for the tip position.

4 Experimental Results

The method developed in this paper is used in this section to control the tip position of two flexible arms. The description and identification of both arms may be found in Feliu et al. [4]. The first arm is a minimum phase flexible beam, and the second is a non-minimum phase flexible arm.

4.1 Experimental Setup

The mechanical system consists of a dc motor, a slender link attached to the motor hub, and a mass at the end of the link floating on an air table. Figure 4 shows the major parts of the system. The link is a piece of music wire (7 inches long and 0.032 inch in diameter) clamped in the motor hub. The tip mass is a 1/16 inch thick, 5 $\frac{3}{4}$ inch diameter fiberglass disk attached at its center to the end of the link with a freely pivoted pin joint. The disk has a mass of 54 grams and floats on the horizontal air table with minimal friction. Since the mass of the link is small compared to that of the disk, and because the pinned joint prevents generation of torque at the end of the link, the mechanical system, used for the first arm, behaves practically like an ideal, single degree-of-freedom, undamped spring-mass system. For the second arm, the wire is replaced by a longer one, and two free pinned masses are attached, one at the middle and the other at the end of the wire. The second system has the characteristic of a flexible arm with distributed masses and is of non-minimum phase type.

A direct drive motor drives the link. The motor is powered by a 40V power supply through a DC servo amplifier. The amplifier current limit is set to 4.12 amps., which corresponds to 9 lb. inch motor torque. Coulomb friction of the motor is about 0.288 lb. inch (corresponding to 0.132 amps) and has a significant effect on the control when the torque applied to the arm is low, as with our slender arm. The system was designed to a give tip response that is much slower than the motor response. Mechanical stops limit the travel of the motor and the hub to about ± 27 degrees.

Two sensors are used for the control of the system. A 7/8 inch, 360 degree potentiometer provides the angle of the motor shaft. A Hamamatsu tracking camera (with an infrared filter) senses the X-Y position of an infrared LED mounted on the tip of the arm. The workspace of the arm is limited to about ± 3 inch (± 25 degrees) by the field of view of the camera.

The control algorithm is implemented on an MC68000-based computer with 512K bytes of dynamic RAM and a 10 MHz clock. Analog interfacing is provided with 12 bit A/D and D/A boards. Switch signals for starting and stopping control routines, as well as other functions, are read through parallel I/O ports. As floating point operations are slow (approximately 0.5 msec. per multiplication), real-time computations are done in integer (approximately 0.08 msec. per multiplication) or short integer (0.02

msec.) arithmetic. A matrox graphics interface card permits the display of data on a 12 inch monitor.

4.2 Single-Mass Flexible Arm

Using an identification technique described in Feliu et al. [4], the parameters of the single-mass flexible arm shown in Figure 5 are given by

J = 0.005529 lb.$in.sec^2$
V = 0.01216 lb.in./rad./sec.
K = 2.184 lb.in./amp.
Coulomb friction = 0.2883 lb.in (0.132 amp.)
$C_t(t)$ = C$(\theta_m(t) - \theta_t(t))$
C = 0.674 lb.in./rad..

The estimated value of the Coulomb friction corresponds to an equivalent torque generated by a beam deflection of 25 degrees, so its effect is very noticeable. Using these parameters, the transfer functions of the motor (assuming that the Coulomb friction has been compensated) and the beam are given by

$$G_m(s) = \frac{394.94(s^2 + 43.75)}{s(s^3 + 2.26s^2 + 165.7s + 103.56)} \tag{10}$$

$$G_b(s) = \frac{43.75}{s^2 + 43.75} \ . \tag{11}$$

4.2.1 Inner loop control design

The inner loop incorporates compensation terms for Coulomb friction and the coupling between the motor and the beam, according to (2). The scheme of Figure 2 is used for the inner loop. A delay term is included in the scheme to take into account the delay in the control signal because of the computations. A sampling period of 3 msec. is used for this inner loop.

An optimization program was developed to get the best controllers using the model obtained for the motor. The settling time (considering an error of less than 1%) of the response of the motor to step commands in the motor angle reference input was minimized. The saturation limit of the current amplifier was also taken into account in this design. Step inputs were assumed as references for the inner loop because, in order to get a good control action, the command angle for the motor should experience very sharp changes. In fact, in our experiments, the motor angle varied much faster than the angle of the tip. The resulting controllers were $G_{c1}(z) = 17.442 - 2.442z^{-1}$ and $G_{c2}(z) = 6.667 - 5.667z^{-1}$.

Figure 6 shows the response of the motor position to a step change in its reference keeping the tip of the arm fixed in the zero angle position. This means that, in the steady-state of this experiment, there is always a coupling torque ,C_t, caused by the bending of 200 mrad existing between the angle of the motor and the angle of the tip. The zero steady-state error shown by the experimental data demonstrates the effectiveness of compensation achieved for the Coulomb friction and for the coupling of the motor with the beam. The settling time achieved for the motor is 33 msec. which is significantly faster than the dynamics of the beam. This allows us to assume that the equivalent transfer function of the inner loop is 1.

4.2.2 Outer loop control design

A simple model-based portion of the control law partitioning scheme was implemented by closing a positive unity gain feedback loop around the tip position and premultiplying by $1/\omega_n^2$. An analog PD servo controller was designed and then discretized using the Tustin transform (VanLandingham [8]). The pulse transfer function of the digital controller is given by

$$G_{c3}(z) = 3281.25(\frac{1 - 0.987z^{-1}}{1 - 0.74z^{-1}}) \ . \tag{12}$$

Figure 7 shows the tip position response to the parabolic trajectory.

4.3 Two-Mass Flexible Arm

This system is similar to the single-mass system, with two concentrated masses spaced along the flexible beam as shown in Figure 8. The transfer function of the beam was found to be

$$\frac{\theta_t(s)}{\theta_m(s)} = \frac{-45.475(s^2 - 1273.3)}{s^4 + 1637.1s^2 + 57903.3175} \ . \tag{13}$$

and the coupling torque between the beam and the motor (expressed in normalized units) as

$$C_t(s) = 1.941\frac{1 + .0013s^2}{1 + .0005943s^2}(\theta_m(s) - \theta_t(s)) \tag{14}$$

4.3.1 Inner Loop Control

It was shown in Feliu et al. [5] that the friction torque for the motor for two-mass flexible arm remained the same as the single-mass flexible arm but the coupling term given by equation (14) is more complex. Since we are using a microprocessor with limited computational capability and the sampling period is 3 msec., a simpler coupling torque $C_t(s) = 1.941(\theta_m(s) - \theta_t(s))$ was used in the implementation. The rest of control scheme for the inner loop of the two-mass arm is the same as the inner loop control of the single-mass arm.

Figure 9 shows the response of the motor to a step change in its reference keeping the tip of the arm fixed in the zero angle position. The response is significantly faster than the dynamics of the beam. This allows us to assume the overall transfer function of the motor to be unity for the design of the outer loop.

4.3.2 Outer Loop Control Design

Using the results of section 3.2.2, a feedforward term for the two-mass flexible arm was obtained as shown in Figure 10. A simple PD servo controller was also designed in the s-plane and then discretized. The pulse transfer function of the digital controller is also shown in the Figure 10.

Figure 11 shows the fourth order parabolic trajectory and the reference input for the tip position. A reference trajectory obtained for maximum acceleration was applied to the tip position control system and its response is shown in Figure 12. For trajectory having acceleration less than the maximum acceleration, the error between the reference and the actual position of the tip will be less than that shown in Figure 12.

5 CONCLUSIONS

Tip position control of lightweight flexible arms in the presence of joint friction is presented in this paper. The control scheme consists of two nested feedback loop, an inner loop to control the position of the motor and an outer loop to control the tip position of the flexible arm. Effects of friction are removed by closing a high gain inner loop. The design of the inner loop which was developed in an earlier paper [3] includes compensation for the coupling torque and the Coulomb friction.

A new method for the design of the outer loop is presented in this paper. First, the dynamics of the beam are simplified using a model-based controller. This controller contains a unity gain positive feedback loop around the tip position to compensate for the first vibration mode. For flexible beams with one vibration mode, this is then pre-multiplied by a gain factor, $1/\omega_n^2$, to reduce the dynamics to a double integrator. For beams with more than one vibration mode, the unity gain positive feedback loop is pre-multiplied by a transfer function containing the inverse of the minimum-phase portion of the loop transfer function. A simple servo/feedforward controllers are then designed for the simplified systems. Nominal trajectory and the feedforward terms are designed by taking into account whether the system is minimum or non-minimum phase. The feedforward term, which is based on the dynamics of the simplified system, is much simpler than the term generated for the existing methods. This makes the control scheme computationally efficient.

The control scheme developed in this paper was applied to a class of lightweight flexible arms, a single-mass minimum phase system and a two-mass non-minimum phase system. Controllers designed here are simpler and provide fast and precise control of the tip. The control scheme also proved to be quite insensitive to noise in the measurement, and to error in modelling.

References

[1] Robert H. Cannon and E. Schmitz, "Precise Control of Flexible Manipulators", Robotics Research, 1985. Journal of Robotics Research, Vol. 6, No. 4, Winter 1987.

[2] P. K. Khosla and T. Kanade, "Experimental Evaluation of Nonlinear Feedback and Feedforward Control Schemes for Manipulators", International Journal of Robotics Research, Vol. 7, No. 1, 1988. Dynamics, Vol. 5, No.4, July-August 1982.

[3] Kuldip S. Rattan, V. Feliu and H. B. Brown, "A Robust Control Scheme for a Single-Link Flexible Manipulator with Friction in the Joints", Proceedings 2nd Annual USAF/NASA Workshop on Automation and Robotics, Dayton, June 1988.

[4] V. Feliu, Kuldip S. Rattan and H. B. Brown, "Model Identification of a Single-Link Flexible Manipulator in the Presence of Friction", Proceedings of 19th ISA Annual Modelling and Simulation Conference, Pittsburgh, May 1988.

[5] V. Feliu, Kuldip S. Rattan and H. B. Brown, "A New Approach To Control Single-Link Flexible Arm. Part II: Control of the Tip Position in the Presence of Joint Friction", Technical Report No. CMU-RI-TR-14 , Robotics Institute, Carnegie Mellon University, Pittsburgh, Pennsylvania 15213.

[6] J. J. Craig, Introduction to Robotics: Mechanics and Control, Addision-Wesley Publishing Company, 1986.

[7] B. C. Kuo, Automatic Control Systems, Prentice-Hall, 1982.

[8] H. F. VanLandingham, Introduction to Digital Control Systems, MacMillan Publishing Company, 1985.

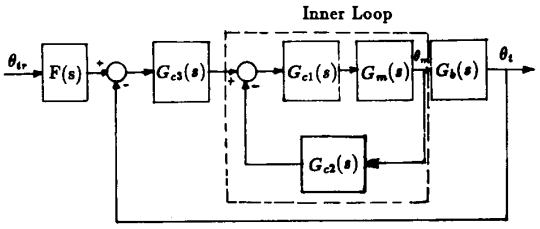

Figure 1. General Robust Control Scheme for Flexible Manipulators.

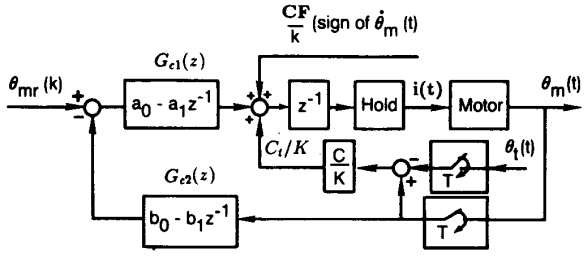

Figure 2. Inner Loop (Motor Position) Control System.

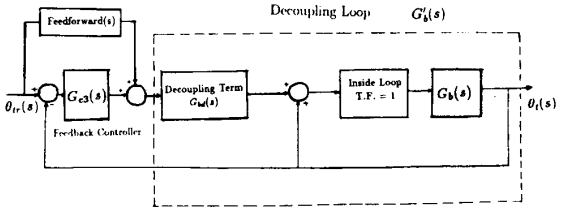

Figure 3. Block Diagram of the Outer Loop (Tip Position) Control Scheme.

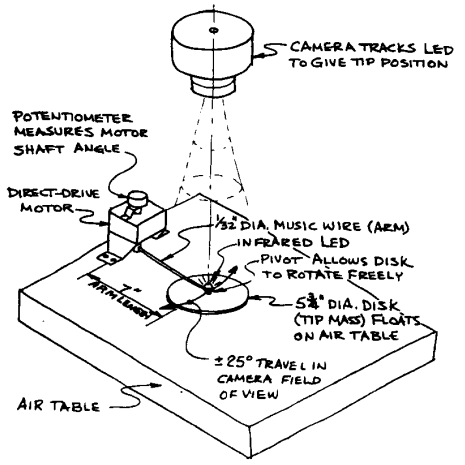

Figure 4. Experimental Setup of the Single-Mass Flexible Arm.

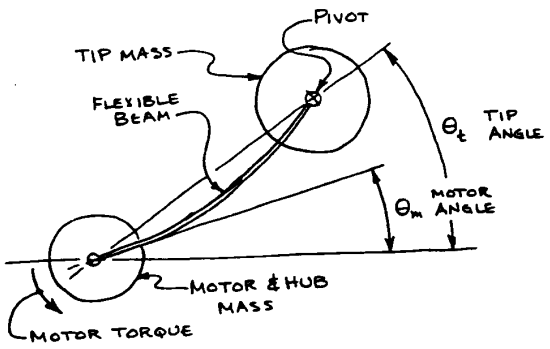

Figure 5. System Nomenclature for the Single-Mass Flexible Arm.

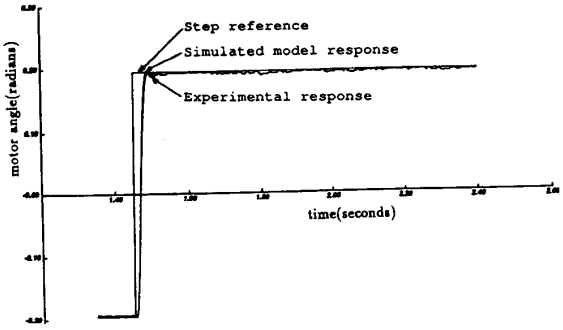

Figure 6. Experimental Response of the motor position to Step Input (Single-Mass Flexible Arm).

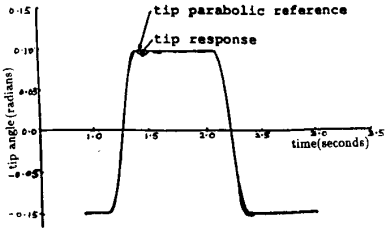

Figure 7. Experimental Tip Response of the Single-Mass Flexible Arm.

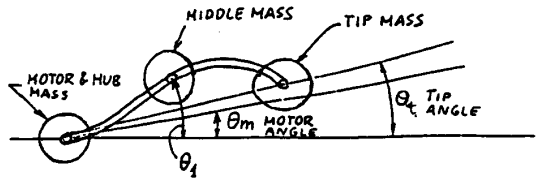

Figure 8. System Nomenclature for the Two-Mass Flexible Arm.

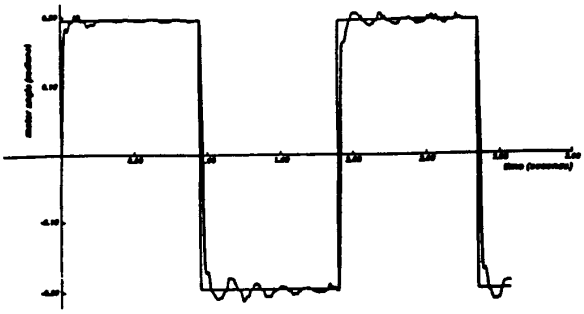

Figure 9. Experimental Response of the Motor Position Control Loop (Two-Mass Arm).

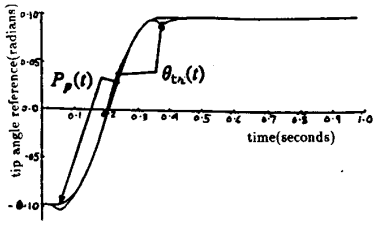

Figure 11. Quasi-Parabolic Trajectory and Optimized Tip Position Reference in the case of Two-Mass Flexible Arm.

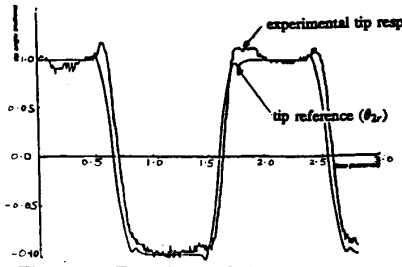

Figure 12. Experimental Tip Position Response of the Two-Mass Flexible Arm.

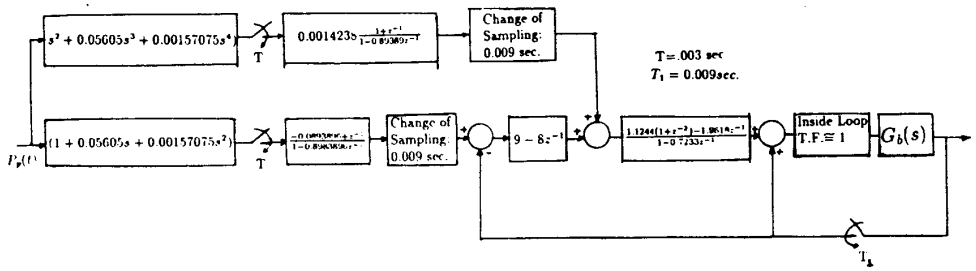

Figure 10. Digital Control for the Outer Loop as Implemented (Two-Mass Flexible Arm).